Self-Assembly

Deutsche Ausgabe: DOI: 10.1002/ange.201412215
Internationale Ausgabe: DOI: 10.1002/anie.201412215

Surface-Induced Selection During In Situ Photoswitching at the Solid/Liquid Interface**

Sara Bonacchi, Mohamed El Garah, Artur Ciesielski, Martin Herder, Simone Conti, Marco Cecchini, Stefan Hecht,* and Paolo Samorì**

Abstract: *Here we report for the first time a submolecularly resolved scanning tunneling microscopy (STM) study at the solid/liquid interface of the in situ reversible interconversion between two isomers of a diarylethene photoswitch, that is, open and closed form, self-assembled on a graphite surface. Prolonged irradiation with UV light led to the in situ irreversible formation of another isomer as by-product of the reaction, which due to its preferential physisorption accumulates at the surface. By making use of a simple yet powerful thermodynamic model we provide a quantitative description for the observed surface-induced selection of one isomeric form.*

In the last two decades the design and synthesis of sophisticated building blocks programmed to interact through noncovalent forces made it possible to construct with a subnanometer precision various self-assembled systems and materials possessing tunable chemical and physical properties.[1] In particular, supramolecular chemistry provides exquisite control over molecular self-assembly,[2] which combines reversibility, directionality, specificity, and cooperativity.[1d,3] In the past few years there has been an increasing effort toward the fabrication of functional supramolecular architectures with a nanoscale control over their mechanical movement, aiming at the development of molecular machines and switches.

Molecular switches, when designed ingeniously, can be fuelled at surfaces by nature's most abundant and powerful energy source—light. The respective photochromic systems are small organic molecules, which are capable of undergoing efficient and reversible photochemical isomerization between two or more (meta)stable states featuring markedly different properties. Among photochromic systems, diarylethenes have been extensively studied because the two isomers (open and closed) are both thermodynamically stable and the cyclization reaction is very fast as it occurs on the picoseconds timescale.[4] In addition, upon photoisomerization diarylethenes exhibit not only a dramatic change in their electronic properties (i.e., orbital energies and electronic transitions) suitable for (opto)electronic devices, such as memories[5] and switches,[6] but they also show a significant change in their conformational flexibility/rigidity, which provides remote control over their molecular organization at surfaces.

Scanning tunneling microscopy (STM) is an established tool to investigate structures and numerous physical and chemical properties of molecules at surfaces with a subnanometer spatial resolution.[7] Its use to explore molecular physisorption at interfaces is particularly appealing as it makes it possible to explore in situ and in real-time dynamic processes including chemical reactions[8] and switching processes.[9] Diarylethene-based self-assembled monolayers in their open and closed forms were previously explored by STM;[10] however, to the best of our knowledge, the in situ reversible interconversion between the two switching states, that is, ring-open and ring-closed isomers, has never been resolved by STM with high-resolution imaging.

Here, we report for the first time a submolecularly resolved STM investigation of the in situ light-induced interconversion between both ring-open and ring-closed diarylethenes at the solid/liquid interface. We have focused our attention on 1,2-bis(2-methyl-5-(4-octadecyloxycarbonylphenyl)thien-3-yl)cyclopent-1-ene (**DAE**, Figure 1a). The presence of long aliphatic side chains in the *para*-positions of both terminal phenyl rings was expected to promote the molecular physisorption on highly oriented pyrolitic graphite (HOPG). Since the interactions between molecules and the HOPG surface are of van der Waals type,[7a,9g] they offer an interesting dynamic scenario characterized by potential exchange based on desorption and re-adsorption.[8h]

To verify that the intrinsic photoswitching ability of the **DAE** was maintained, absorption spectra of the ring-open isomer **DAE-o** (for synthesis and characterization see the

[*] Dr. S. Bonacchi,[+] Dr. M. El Garah,[+] Dr. A. Ciesielski, Prof. Dr. P. Samorì
Nanochemistry Laboratory, ISIS & icFRC
Université de Strasbourg & CNRS
8 allée Gaspard Monge, 67000 Strasbourg (France)
E-mail: samori@unistra.fr
M. Herder, Prof. Dr. S. Hecht
Department of Chemistry, Humboldt-Universität zu Berlin
Brook-Taylor-Str. 2, 12489 Berlin (Germany)
E-mail: sh@chemie.hu-berlin.de
S. Conti, Dr. M. Cecchini
Laboratory of Molecular Function and Design, ISIS & icFRC
Université de Strasbourg & CNRS
8 allée Gaspard Monge, 67000 Strasbourg (France)
E-mail: mcecchini@unistra.fr
[+] These authors contributed equally to this work.

[**] This work was supported by the EC through the Marie Curie IEF GALACTIC (PIEF-GA-2014-628563), the ERC projects SUPRAFUNCTION (GA-257305) and Light4Function (GA-308117), the Agence Nationale de la Recherche through the LabEx project Chemistry of Complex Systems (ANR-10-LABX-0026_CSC), the International Center for Frontier Research in Chemistry (icFRC) as well as the German Research Foundation (DFG through SFB 658). S.C. thanks the University of Strasbourg (IdEX program Nr. 16141) for his PhD fellowship.

Supporting information for this article is available on the WWW under http://dx.doi.org/10.1002/anie.201412215.

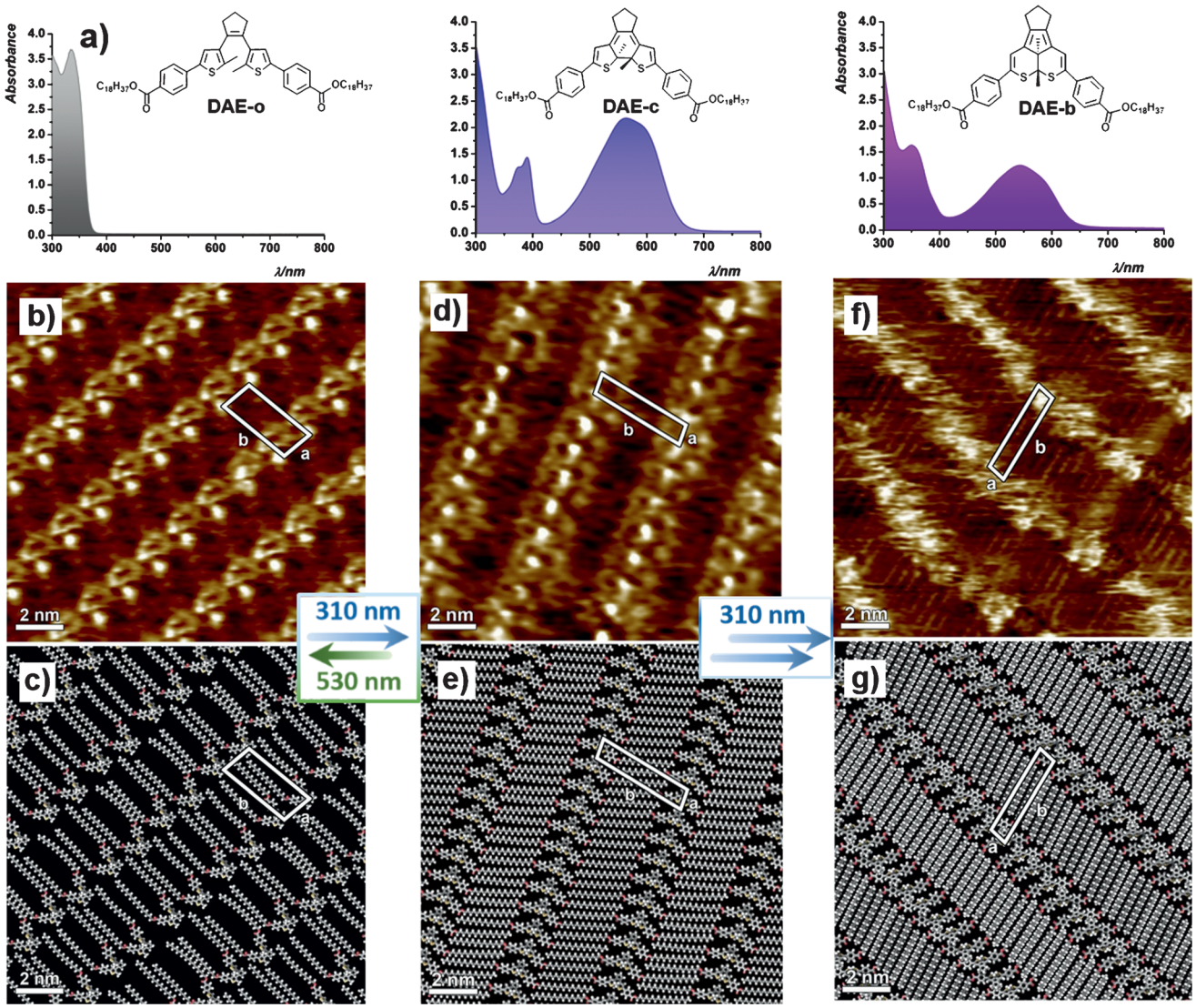

Figure 1. a) Chemical structures and UV/Vis spectra of investigated diarylethene in its open (**DAE-o**), closed (**DAE-c**), and closed containing 60% of (irreversible) by-product (**DAE-b**) form. Height STM images of monolayers of b) **DAE-o**, d) **DAE-c**, and f) **DAE-b** at the liquid/graphite interface self-assembled from solution in 1-phenyloctane (tunneling parameters: average tunneling current (I_t) = 25–30 pA, bias voltage $-650\ \text{mV} \leq V_t \leq -400\ \text{mV}$). Minimized molecular packing motifs of c) **DAE-o**, e) **DAE-c**, and g) **DAE-b** (see molecular modeling in SI for details).

Supporting Information, SI) were recorded in 1-phenyloctane solution (Figure 2 a,c). UV irradiation (310 nm) generates a new absorption band in the visible part of the spectrum (at ca. 560 nm), which constitutes a characteristic footprint of the closed-ring isomer (**DAE-c**). Upon visible-light irradiation (530 nm), the **DAE-c** was converted back to **DAE-o** and its original spectrum was restored. Noteworthy, the isosbestic point at 363 nm remains throughout the entire irradiation, ruling out the appearance of side products in solution during the photoisomerization cycle upon light exposure up to about several tens of minutes (see Figures S1 and S2).

Initially, we investigated the self-assembly of **DAE-o** by applying a drop of a 0.5 mM solution of **DAE-o** in 1-phenyloctane onto the HOPG surface. The STM image of the obtained monolayer (Figures 1 b and S3) showed a crystalline structure that consists of lamellar architectures. The observed crystalline domains exhibit a unit cell: $a = (1.5 \pm 0.1)$ nm, $b = (3.4 \pm 0.1)$ nm, $\alpha = (79 \pm 2)°$ leading to an area $A = (5.0 \pm 0.1)\ \text{nm}^2$, in which each unit cell contains one molecule **DAE-o** (Figure 1 c). In this 2D crystal, because of the steric hindrance between thienyl groups, the cores of **DAE-o** are partially physisorbed on the surface and adopt U-shape conformation. Furthermore, the octadecyl side chains are most likely physisorbed flat on the surface adopting a parallel conformation, that is, with both alkyl chains pointing toward the same direction, although due to their high conformational dynamics they could not be resolved with STM.

As for DAEs only the antiparallel conformation is photoactive;[11] ring-closure cannot be induced within the monolayer but only in solution. The stability of the crystalline monolayer, on the time scale of several minutes, and the

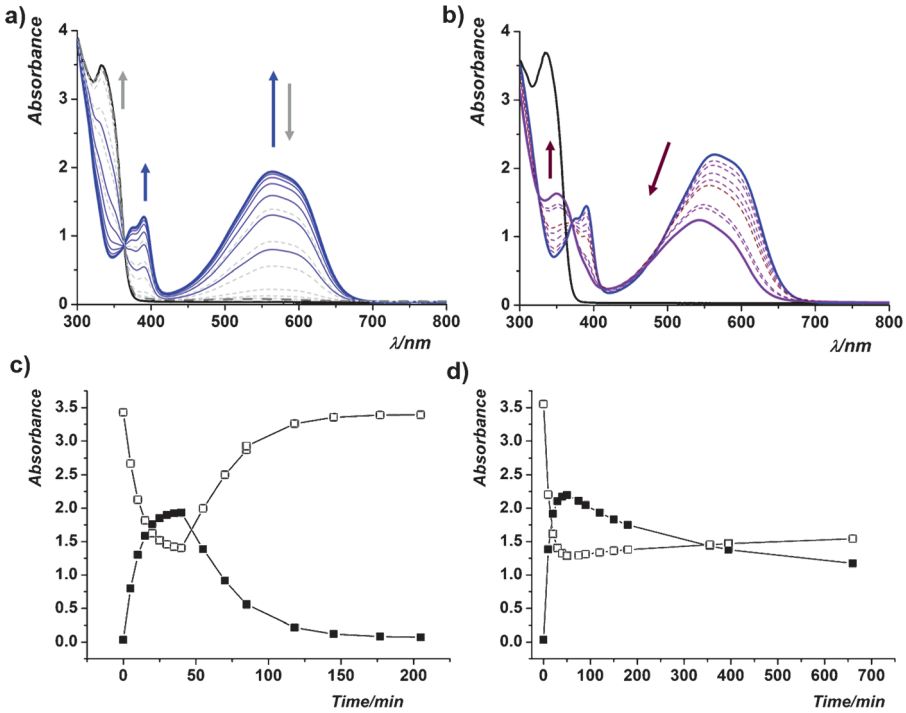

Figure 2. Photochromic behavior of DAE in solution: UV/Vis absorption spectra of **DAE** ($c = 0.5$ mM) in cyclohexane/1-phenyloctane (1:5) during a) the course of UV and visible irradiation ($\lambda_{irr} = 310$ nm and 530 nm, respectively) from the ring-open isomer **DAE-o** to the photostationary state, consisting almost exclusively of the ring-closed isomer **DAE-c**, and back. b) Formation of the by-product **DAE-b** upon continuing UV irradiation ($\lambda_{irr} = 310$ nm) of **DAE-c**. c) and d) time-dependent absorption changes at 330 nm (empty squares) and at 560 nm (full squares) during the (a) and (b) isomerization studies, respectively.

possibility to record highly resolved images indicates that the molecules are immobilized on the surface, that is, the supramolecular motif is stabilized by relatively strong molecule–graphite van der Waals interactions.

STM was used to probe the in situ photoisomerization of **DAE-o** self-assembled structures, by irradiation with UV light. To this end, the preexisting monolayer of **DAE-o** was irradiated for 5 min with UV light (310 nm). In all experiments we have performed, the irradiation of **DAE-o** monolayers resulted in the desorption of **DAE-o** molecules followed by the molecular readsorption to form a new type of 2D crystalline motif (Figure 1 d). This new 2D pattern exhibits unit cell parameters: $a = (1.0 \pm 0.1)$ nm, $b = (4.1 \pm 0.1)$ nm, $\alpha = (79 \pm 2)°$ leading to an area $A = (4.0 \pm 0.1)$ nm^2, in which each unit cell contains one molecule (Figure 1 e). Noteworthy, the unit cell parameters of this crystalline structure are in perfect agreement with those extracted from STM images of monolayers obtained from **DAE-c** molecules obtained by ex situ irradiation of **DAE-o** solution (see Figures S7 (**DAE-o**) and S8 (**DAE-c**)). In the STM images one can notice three bright features linearly aligned to the main lamellar axis which can be assigned to the two phenyl rings and to the core of the **DAE-c** molecules, the latter appearing brighter due to its extended π-conjugation. Importantly, the **DAE-c** monolayers can be converted in situ back to the **DAE-o** motif if irradiated with 530 nm light for 20 min (Figures S2 and S6). Hence, irradiation of **DAE-c** monolayers with green light resulted in desorption followed by the readsorption of **DAE-o** in its favored self-assembly structure.

According to the previous reports[12] and in line with recent investigations by some of us,[13] a prolonged UV irradiation of diarylethenes can induce the formation of a photoirreversible by-product, composed of an annulated polycyclic core (as shown for **DAE-b** in Figure 1 a, right).[10c,d] Interestingly, a longer in situ UV irradiation of both the **DAE-o** and **DAE-c** monolayers ($t > 20$ min and 6 min, respectively) resulted in an unexpected and different 2D assembly (Figures 1 f, S5, and S6) on graphite. This new assembly pattern exhibits unit cell parameters: $a = (0.9 \pm 0.3)$ nm, $b = (4.0 \pm 0.5)$ nm, $\alpha = (79 \pm 2)°$ leading to an area $A = (3.5 \pm 0.5)$ nm^2, in which each unit cell contains one diarylethene molecule. In this 2D crystal, interdigitated octadecyl chains are clearly visible in the STM image. The brighter parts of the STM image can be assigned to the polycyclic core of the by-product molecules; the fuzzy contrast strongly suggests that these cores do not interact strongly with the underlying HOPG surface. It is indeed most likely that the core of the molecules is located out-of-plane with respect to the octadecyl side chains; therefore their conformational mobility is extremely high during STM mapping resulting in fuzzy areas in STM pictures. Noteworthy, irradiation of this new type of monolayer with either blue and/or green light did not alter the packing motif, indicating that the molecules cannot be switched back either to the open or to the closed form. In light of these findings, we can ascribe the observed 2D motif in the STM images (Figure 1 f) to the by-product form of diarylethene, that is, **DAE-b**.

To confirm the presence of the **DAE-b** on the HOPG substrate, we investigated, ex situ, the photophysical properties of the **DAE-o** solution under UV light (Figures 2 b, S1, and S2). As expected,[10c,d] the absorption maximum of the by-product is slightly blue-shifted (540 nm) and broader when compared to the **DAE-c** form. The quantity of by-product formed starting from a **DAE-c** solution depends on the time of irradiation, being up to a 60% in content after 10 h (Figure 2 d). Noteworthy, the self-assembled motif in 2D monitored on samples prepared by applying a drop of the ex situ prepared **DAE-b** to HOPG perfectly matches with the one observed after a prolonged UV irradiation in situ (Figure S9).

The coexistence of the by-product and the ring-closed isomer in the solution makes it interesting to explore their

self-assembly on graphite in the framework of competitive physisorption at the solid/liquid interface. By applying a drop of a mixture consisting mostly of the ring-closed isomer (**DAE-c**/**DAE-b** = 92:8), only patterns of the by-product were found by STM, which indicates a surface-induced selection of the by-product. Importantly, the selective adsorption observed here allows for the enrichment (and potential removal) of the minor by-product of the photochemical reaction in solution.

To gain a more quantitative understanding of the surface selectivity for the by-product, we performed a simple thermodynamic analysis of the 2D self-assembly of the open, the closed, and the by-product isomers on graphene. To this end, the free energy cost of covering a given surface area of substrate was estimated by modeling the self-assembly of freely diffusing monomers in the gas phase to defect-free crystalline architectures on graphene.[14] In this model, the energy of forming the 2D nanopattern includes contributions from both molecular adsorption (E_{ads}) and intermolecular interaction in the self-assembled monolayer (E_{inter}). These terms were evaluated here using the GAFF force field[15] and 2D model architectures with an atomistic representation of the graphene surface.[16] In addition, the entropic cost associated to 2D confinement and assembly into a crystalline architecture was evaluated using a statistical mechanics approach based on the ideal gas approximation (see the molecular modeling in SI). In this framework, the free energy excess on self-assembly normalized per unit cell area (γ) was evaluated and used as a quantitative measure to compare the (relative) thermodynamic stability of the three architectures in Figure 1.

The results obtained for the open, closed, and by-product isomers clearly show that at the experimental conditions (0.5 mM concentration in solution) the **DAE-b** architecture is most stable with $\gamma = -34.61$ kcal mol^{-1} nm^{-2}, followed by **DAE-c** and **DAE-o** in this order (Table 1). The density of packing is primarily responsible for the difference in free energy between the open form and the others, that is, the higher the density the higher the energetic gain per surface area. The physisorption of the by-product is preferred over that of the closed isomer as a result of opposing contributions. On one hand, the adsorption energy per **DAE-b** molecule is weaker by 11.4 kcal mol^{-1} if compared to **DAE-c**. On the other hand, the higher packing density of **DEA-b** molecules results in intermolecular interactions in the monolayer enhanced by 13.5 kcal mol^{-1} per unit cell. As shown in Figure 3, the core of the diarylethene derivatives is face-on in the **DAE-c** architecture, whereas it is edge-on in the **DAE-b**. Moreover, whereas in the former the octadecyl chains are physisorbed in an in-plane zig-zag fashion, in the latter they adopt an out-of-plane conformation. Overall, the interplay between E_{ads} and E_{inter}, which is quantified by the energy per unit cell (E_{uc}) in Table 1, is in favor of the **DAE-b** architecture by 4.5 kcal mol^{-1}. In addition, because the entropic cost of association at the experimental conditions is similar for these two architectures ($\Delta\Delta S < 1$ kcal mol^{-1} nm^{-2}, see SI), the **DAE-b** nanopattern is predicted to be thermodynamically preferred. This interpretation rationalizes all STM observations, yields atomistic models for the **DAE** self-assembled architectures, and provides new insight on the nature of the surface-induced selection and amplification of the photoirradiation by-product. Despite the higher free energy of the open versus the closed isomeric architecture amounting to −21.04 and −30.83 kcal mol^{-1} nm^{-2}, respectively, it is interesting to note that STM imaging reveals that upon illumination of the closed monolayer with visible light a reorganization

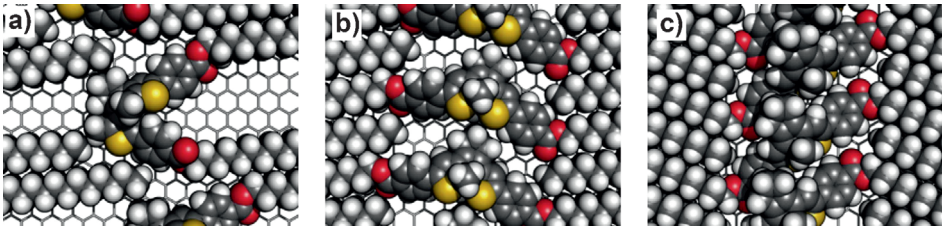

Figure 3. Magnification of architectures for the a) **DAE-o**, b) **DAE-c**, and c) **DAE-b** isomers obtained by molecular modeling. Note the parallel conformation of **DAE-o**, the different packing of **DAE-c** and **DAE-b** due to their different alkyl chain conformations, and the overlap of the cores in **DAE-b**, which is not present in **DAE-c**.

Table 1: Experimental and modeled unit cell parameters for the three **DAE** isomers and their estimated thermodynamic quantities. E_{ads} is the adsorption energy, E_{inter} the interaction energy with the neighboring molecules, E_{uc}/A the total energy per molecule normalized by the unit cell area, and γ the free energy excess considering both energetic and entropic contributions.

		a [nm]	*b* [nm]	α [°]	*A* [nm^2]	E_{ads} [kcal mol^{-1}]	$E_{inter}/2$ [kcal mol^{-1}]	E_{uc}/A [kcal mol^{-1} nm^{-2}]	γ [kcal mol^{-1} nm^{-2}]
DAE-o	theoretical	1.5	3.4	76	4.9	−119.1	−15.7	−26.38	−21.04
	experimental	(1.5 ± 0.1)	(3.4 ± 0.1)	(79 ± 2)	(5.0 ± 0.1)				
DAE-c	theoretical	0.9	4.2	78	3.8	−112.7	−32.6	−38.14	−30.83
	experimental	(1.0 ± 0.1)	(4.1 ± 0.1)	(79 ± 2)	(4.0 ± 0.1)				
DAE-b	theoretical	0.9	3.9	78	3.4	−101.3	−46.1	−42.60	−34.61
	experimental	(0.9 ± 0.3)	(4.0 ± 0.5)	(79 ± 2)	(3.5 ± 0.5)				

into the open monolayer is observed. This indicates that the conversion from **DAE-c** to **DAE-o** on graphite is quantitative in line with the behavior observed in solution.

In summary, a novel diarylethene derivative has been designed and synthesized. It exhibits pronounced affinity for the graphite surface in all its isomeric forms, thereby providing for the first time a high-resolution evidence of the in situ reversible light-powered switching of a diarylethene between the open and the closed form at the solid/liquid interface. Prolonged irradiation with UV light of both the "wet" film and the solution led to the irreversible formation of the annulated isomer (photochemical by-product). A simple yet insightful thermodynamic analysis of the self-assembly provided evidence for the capacity of the surface to act as a selector, thereby amplifying the presence of the minor constituent on the surface starting from a mixture. Such an ability of graphite to behave as a filter or selector opens new perspectives toward the use of graphene as stationary phase in liquid chromatography and more generally to exploit surface selectivity to purify multicomponent solutions.

Keywords: diarylethene · in situ photoswitching · interfaces · scanning tunneling microscopy · self-assembly

How to cite: *Angew. Chem. Int. Ed.* **2015**, *54*, 4865–4869
Angew. Chem. **2015**, *127*, 4947–4951

[1] a) J.-M. Lehn, *Science* **1993**, *260*, 1762–1763; b) J. H. van Esch, B. L. Feringa, *Angew. Chem. Int. Ed.* **2000**, *39*, 2263–2266; *Angew. Chem.* **2000**, *112*, 2351–2354; c) J. A. A. W. Elemans, A. E. Rowan, R. J. M. Nolte, *J. Mater. Chem.* **2003**, *13*, 2661–2670; d) F. J. M. Hoeben, P. Jonkheijm, E. W. Meijer, A. P. H. J. Schenning, *Chem. Rev.* **2005**, *105*, 1491–1546; e) V. Palermo, P. Samorì, *Angew. Chem. Int. Ed.* **2007**, *46*, 4428–4432; *Angew. Chem.* **2007**, *119*, 4510–4514; f) L. C. Palmer, S. I. Stupp, *Acc. Chem. Res.* **2008**, *41*, 1674–1684; g) Q. W. Li, W. Y. Zhang, O. S. Miljanic, C. H. Sue, Y. L. Zhao, L. H. Liu, C. B. Knobler, J. F. Stoddart, O. M. Yaghi, *Science* **2009**, *325*, 855–859.

[2] C.-A. Palma, M. Cecchini, P. Samorì, *Chem. Soc. Rev.* **2012**, *41*, 3713–3730.

[3] a) G. M. Whitesides, J. P. Mathias, C. T. Seto, *Science* **1991**, *254*, 1312–1319; b) J.-M. Lehn, *Supramolecular chemistry: concepts and perspectives*, VCH, New York, **1995**.

[4] a) H. Miyasaka, T. Nobuto, A. Itaya, N. Tamai, M. Irie, *Chem. Phys. Lett.* **1997**, *269*, 281–285; b) M. Irie, T. Fukaminato, K. Matsuda, S. Kobatake, *Chem. Rev.* **2014**, *114*, 12174–12277.

[5] R. C. Shallcross, P. Zacharias, A. Köhnen, P. O. Körner, E. Maibach, K. Meerholz, *Adv. Mater.* **2013**, *25*, 469–476.

[6] E. Orgiu, N. Crivillers, M. Herder, L. Grubert, M. Paetzel, J. Frisch, E. Pavlica, D. T. Duong, G. Bratina, A. Salleo, N. Koch, S. Hecht, P. Samorì, *Nat. Chem.* **2012**, *4*, 675–679.

[7] a) S. De Feyter, F. C. De Schryver, *Chem. Soc. Rev.* **2003**, *32*, 139–150; b) F. Rosei, M. Schunack, Y. Naitoh, P. Jiang, A. Gourdon, E. Laegsgaard, I. Stensgaard, C. Joachim, F. Besenbacher, *Prog. Surf. Sci.* **2003**, *71*, 95–146; c) J. V. Barth, G. Costantini, K. Kern, *Nature* **2005**, *437*, 671–679; d) L. Grill, *J. Phys. Condens. Matter* **2008**, *20*, 053001; e) K. Müllen, J. P. Rabe, *Acc. Chem. Res.* **2008**, *41*, 511–520; f) A. Ciesielski, C.-A. Palma, M. Bonini, P. Samorì, *Adv. Mater.* **2010**, *22*, 3506–3520.

[8] a) N. A. A. Zwaneveld, R. Pawlak, M. Abel, D. Catalin, D. Gigmes, D. Bertin, L. Porte, *J. Am. Chem. Soc.* **2008**, *130*, 6678–6679; b) J. A. Lipton-Duffin, J. A. Miwa, M. Kondratenko, F. Cicoira, B. G. Sumpter, V. Meunier, D. F. Perepichka, F. Rosei, *Proc. Natl. Acad. Sci. USA* **2010**, *107*, 11200–11204; c) J. M. Cai, P. Ruffieux, R. Jaafar, M. Bieri, T. Braun, S. Blankenburg, M. Muoth, A. P. Seitsonen, M. Saleh, X. L. Feng, K. Mullen, R. Fasel, *Nature* **2010**, *466*, 470–473; d) C.-A. Palma, P. Samorì, *Nat. Chem.* **2011**, *3*, 431–436; e) J. F. Dienstmaier, D. D. Medina, M. Dogru, P. Knochel, T. Bein, W. M. Heckl, M. Lackinger, *ACS Nano* **2012**, *6*, 7234–7242; f) D. den Boer, M. Li, T. Habets, P. Iavicoli, A. E. Rowan, R. J. M. Nolte, S. Speller, D. B. Amabilino, S. De Feyter, J. A. A. W. Elemans, *Nat. Chem.* **2013**, *5*, 621–627; g) J. W. Colson, W. R. Dichtel, *Nat. Chem.* **2013**, *5*, 453–465; h) A. Ciesielski, M. El Garah, S. Haar, P. Kovaricek, J.-M. Lehn, P. Samorì, *Nat. Chem.* **2014**, *6*, 1017–1023.

[9] a) P. Vanoppen, P. C. M. Grim, M. Rucker, S. De Feyter, G. Moessner, S. Valiyaveettil, K. Müllen, F. C. De Schryver, *J. Phys. Chem.* **1996**, *100*, 19636–19641; b) G. Pace, V. Ferri, C. Grave, M. Elbing, C. von Hanisch, M. Zharnikov, M. Mayor, M. A. Rampi, P. Samorì, *Proc. Natl. Acad. Sci. USA* **2007**, *104*, 9937–9942; c) A. S. Kumar, T. Ye, T. Takami, B. C. Yu, A. K. Flatt, J. M. Tour, P. S. Weiss, *Nano Lett.* **2008**, *8*, 1644–1648; d) L. Piot, R. M. Meudtner, T. El Malah, S. Hecht, P. Samorì, *Chem. Eur. J.* **2009**, *15*, 4788–4792; e) D. Bléger, A. Ciesielski, P. Samorì, S. Hecht, *Chem. Eur. J.* **2010**, *16*, 14256–14260; f) A. Ciesielski, S. Lena, S. Masiero, G. P. Spada, P. Samorì, *Angew. Chem. Int. Ed.* **2010**, *49*, 1963–1966; *Angew. Chem.* **2010**, *122*, 2007–2010; g) A. Ciesielski, P. Samorì, *Nanoscale* **2011**, *3*, 1397–1410; h) K. Tahara, K. Inukai, J. Adisoejoso, H. Yamaga, T. Balandina, M. O. Blunt, S. De Feyter, Y. Tobe, *Angew. Chem. Int. Ed.* **2013**, *52*, 8373–8376; *Angew. Chem.* **2013**, *125*, 8531–8534.

[10] a) N. Katsonis, A. Minoia, T. Kudernac, T. Mutai, H. Xu, H. Uji-i, R. Lazzaroni, S. De Feyter, B. L. Feringa, *J. Am. Chem. Soc.* **2008**, *130*, 386–387; b) R. Arai, S. Uemura, M. Irie, K. Matsuda, *J. Am. Chem. Soc.* **2008**, *130*, 9371–9379; c) T. Sakano, Y. Imaizumi, T. Hirose, K. Matsuda, *Chem. Lett.* **2013**, *42*, 1537–1539; d) S. Yokoyama, T. Hirose, K. Matsuda, *Chem. Commun.* **2014**, *50*, 5964–5966.

[11] a) K. Uchida, E. Tsuchida, Y. Aoi, S. Nakamura, M. Irie, *Chem. Lett.* **1999**, 63–64; b) W. Li, C. Jiao, X. Li, Y. Xie, K. Nakatani, H. Tian, W. Zhu, *Angew. Chem. Int. Ed.* **2014**, *53*, 4603–4607; *Angew. Chem.* **2014**, *126*, 4691–4695.

[12] M. Irie, T. Lifka, K. Uchida, S. Kobatake, Y. Shindo, *Chem. Commun.* **1999**, 747–750.

[13] M. Herder, B. M. Schmidt, L. Grubert, M. Pätzel, J. Schwarz, S. Hecht, *J. Am. Chem. Soc.* **2015**, DOI: 10.1021/ja513027s.

[14] S. Haar, A. Ciesielski, J. Clough, H. Yang, R. Mazzaro, F. Richard, S. Conti, N. Merstorf, M. Cecchini, V. Morandi, C. Casiraghi, P. Samorì, *Small* **2014**, DOI: 10.1002/smll.201402745.

[15] J. Wang, R. M. Wolf, J. W. Caldwell, P. A. Kollman, D. A. Case, *J. Comput. Chem.* **2004**, *25*, 1157–1174.

[16] S. Conti, M. Cecchini, *J. Phys. Chem. C* **2015**, *119*, 1875–1879.

Received: December 19, 2014
Published online: February 27, 2015

